Derivation of Residual Noise of Filtered Poisson and Gaussian Series

W. Yao and J.B. Farr

Radiological Sciences, St. Jude Children's Research Hospital, Memphis, USA

Abstract— **Residual noise analysis is useful in designing optimal filters for noise reduction. To begin we derive the variance of residual noise σ_r^2, from Poisson and Gaussian series after filtered by a Gaussian filter. For Poisson series, we have $\sigma_r^2 = \sqrt{2\pi} I^* / (4\sigma_0)$, and for Gaussian series $\sigma_r^2 = \sqrt{2\pi}\sigma^2 / (4\sigma_0)$, where I^* is the noiseless signal in the Poisson series, σ and σ_0 are the standard deviations of the Gaussian series and the Gaussian filter, respectively. Then by utilizing these results, we design an optimal filter with aim to minimizing the local noise-to-signal ratio in a Poisson series with $I^* = 40 + A\sin(kx)$, which can represent the change of contrast and resolution of an image with A and k, respectively.**

Keywords— **Residual noise, optimal filter, image processing.**

I. Introduction

Noise reduction is one of the main practices in image processing and has broad applications in segmentation, registration and so on. Ionizing-radiation imaging systems such as x-ray computed tomography (CT), cone beam CT, and positron emission tomography (PET) have been widely used in diagnosis, image-guided treatment and treatment vilification. Besides the benefit from these medical imaging systems, the potential long term effect of the ionization dose is of concern. Ionization is one of the carcinogens. The probability of radiation induced cancers is proportional to the radiation dose. Use of low dose imaging is desired in clinic practice, but increases the noise-to-signal ratio in the projections and thus reduces the image quality of the reconstructed image.

The goal of noise reduction is to filter out the noise and meanwhile preserve the structures in the original image, so that the processed image can provide acceptable clinical benefit while lowering the exposure risk. Usually, noise reduction is accompanied by structure blurring. In order to better balance de-noising and structure blurring, multi-scale techniques use local structure information and noise property to adjust those parameters in the algorithms or filters[1,2]. Residual noise analysis can be useful for selecting those optimal parameters. To our best knowledge, there is no publication giving the analytical form of the variance of residual noise after a stochastic process is filtered by a Gaussian. In this work, we derive the form of the residual noise from a Gaussian and Poisson processes filtered by a Gaussian. Gaussian and Poisson noises are the most common noise in medical images. Application of the residual noise analysis to designing filters for minimizing noise-to-signal ration is also given.

II. Derivation of the Variance of Residual Noise

A. Gaussian noise

Assume a series of Gaussian noise $\{\eta(x)\}$, x=1, 2, 3, …, being filtered by a flat filter:

$$\rho(x) = \begin{cases} \Delta y & x \in [-x_0, x_0] \\ 0 & \text{otherwise} \end{cases}, \tag{1}$$

where both Δy and x_0 are positive. The result is again a noise series $\{\eta'(x_0)\}$:

$$\eta'(x; x_0) = \frac{\Delta y \int_{x-x_0}^{x+x_0} \eta(t)dt}{\Delta y \int_{x-x}^{x+x_0} dt} = \frac{1}{2x_0}\int_{x-x_0}^{x+x_0} \eta(t)dt \,. \tag{2}$$

Gaussian noise is independent and identically distributed (i.i.d.), i.e., for $Y = \sum_{i=1}^{N} \eta_i$, one has the variance of Y, $\sigma^2(Y) = N\sigma^2(\eta)$. Thus from (2), the variance of the residual noise $\eta'(x_0)$ is

$$\sigma^2(\eta') = \frac{1}{4x_0^2} 2x_0\, \sigma^2(\eta) = \frac{1}{2x_0}\sigma^2(\eta). \tag{3}$$

Namely, the variance of the residual noise decreases as the width of the flat filter.

Further, for a statistically spatially independent noise sequence, it can be treated like a constant when integrated in space. Particularly, following expression holds.

$$\frac{1}{\sqrt{2\pi}\sigma_0}\int_{-\infty}^{\infty} \eta(t)\exp\left(-\frac{(x-t)^2}{2\sigma_0^2}\right)dt = \frac{1}{2\bar{x}}\int_{x-\bar{x}}^{x+\bar{x}} \eta(t)\,dt \,, \tag{4}$$

Where $2\bar{x}$ is the mean width of the Gaussian bell shape

$$2\bar{x} = \frac{1}{\sqrt{2\pi}\sigma_0}\int_{-\infty}^{\infty} 2x\exp\left(-\frac{x^2}{2\sigma^2}\right)dx = \frac{4\sigma_0}{\sqrt{2\pi}} \,. \tag{5}$$

By replacing $2x_0$ in (3) by $2\bar{x}$ in (5), we obtain the variance of residual noise from a Gaussian noise series (with vari-

D.A. Jaffray (ed.), *World Congress on Medical Physics and Biomedical Engineering, June 7-12, 2015, Toronto, Canada*,
IFMBE Proceedings 51, DOI: 10.1007/978-3-319-19387-8_50

ance $\sigma^2(\eta)$) filtered by another Gaussian filter (with property variance σ_0^2) as

$$\sigma_r^2 = \frac{\sqrt{2\pi}\sigma^2(\eta)}{4\sigma_0}. \quad (6)$$

The variance of residual noise is inversely proportional to the standard deviation of the filter. When applying (6) to a pixelated image, we must have $4\sigma_0/\sqrt{2\pi} \geq 1$, otherwise, the truncated filter is wholly within one pixel and thus there is no effect of the filter onto the image.

B. Poisson noise

Again, we consider a Poisson series $I = I^* + \eta$ filtered by a flat filter (1), where I^* is the noiseless constant signal. We have

$$I'(x;x_0) = I^* + \frac{1}{2x_0}\int_{x-x_0}^{x+x_0}\eta(t)dt \quad (7)$$

or

$$2x_0 I'(x;x_0) = 2x_0 I^* + \int_{x-x_0}^{x+x_0}\eta(t)dt. \quad (8)$$

Note that for Poisson noise *I*, the function of $\int_{x-x_0}^{x+x_0} I\,dt$ is equivalent to a counter detector, where the buffering time equals $2x_0$. For a coming Poisson sequence, no matter how long the buffering time is, the signal from the detector is still in Poisson, but the noiseless signal is proportional to the buffering time. For our case, we have

$$\sigma^2\left(2x_0 I'(x;x_0)\right) = 2x_0 I^* = \sigma^2\left(\int_{x-x_0}^{x+x_0}\eta(t)\,dt\right). \quad (9)$$

What we expect is the variance corresponding to I^*. From (7) and (8),

$$\sigma^2\left(I'(x;x_0)\right) = \frac{1}{4x_0^2}\sigma^2\left(\int_{x-x_0}^{x+x_0}\eta(t)dt\right) = \frac{I^*}{2x_0}. \quad (10)$$

Again, for spatially independent noise, the Gaussian filter is equivalent to a flat filter with the mean width given in (5). We obtain the variance of residual noise from a Poisson process after filtered by a Gaussian as

$$\sigma_r^2 = \frac{\sqrt{2\pi}I^*}{4\sigma_0}. \quad (11)$$

The variances of the residual noise in (6) and (11) are the same because for Poisson noise the variance is equal to I^*. This is reasonable because Poisson process can be treated as Gaussian when I^* is sufficiently large.

It is valuable to point out that (a) the result (11) can also be obtained by using the i.i.d. property of a Poisson series, and (b) $\int_{x-x_0}^{x+x_0} I\,dt$ is a Poisson process but $\frac{1}{2x_0}\int_{x-x_0}^{x+x_0}\eta(t)dt$ is not simply because a Poisson process is defined in integers.

III. Application to Minimizing Noise-to-Signal Ratio

Consider performing a Gaussian filter on a Poisson noise fluence consisting of noiseless fluence I^* and noise η

$$\begin{aligned} G\otimes I &= G\otimes I^* + G\otimes\eta \\ &= \left(G\otimes I^* - I^*\right) + I^* + G\otimes\eta, \end{aligned} \quad (12)$$

where $\otimes$ is for convolution operator. The term $G\otimes I^* - I^*$ represents the structure damage and $G\otimes\eta$ the residual noise. Balance of noise reduction and structure preservation can be reached by minimizing following expression,

$$g = \frac{\sigma^2(G\otimes I^* - I^*) + \sigma^2(G\otimes\eta)}{\sigma^2(\eta)}. \quad (13)$$

In case that η is independent on I^*, and $\sigma^2(\eta)$ is replaced by I^* in the denominator, g becomes the noise-to-signal ratio of the filtered projection. For Poisson noise, η is dependent on I^*, but g is still a proper measurement of the filter's performance. Ideally $g = 0$, and in practice $g \in [0,1]$. The term $\sigma^2(\eta)$ in (13) is not relative to filter *G*, but used here to normalize the quantity g when $\sigma_0 = 0$, or no filter is applied. As σ_0 increases from zero, the effect of noise reduction may be larger than that of structure blur, and the value of g decreases until these two effects reach a balance. Further increase of σ_0 will cause g to increase, and in this case, the signal-to-noise ratio (SNR) of the processed image will decrease. By searching the value of g with various values of σ_0, one may numerically obtain optimal σ_0 but the searching can be time consuming.

If the form of I^* is known, we can derive the optimal σ_0 to obtain the filtered series with maximal SNR. In this work, we assume the noiseless signal

$$I^* = I_0 + A\sin(kx), \quad (14)$$

where I_0, A and k are parameters, with following two considerations. (a) (14) may stand for the dominant form of the

local Fourier expansion of an image, and (b) the parameters A and k represent the contrast and resolution of an image respectively, and I_0 represents mAs.

$$\sigma^2\left(G\otimes I^*-I^*\right)=A^2\left[1-\exp(-k^2\sigma_0^2/2)\right]^2\sin^2(kx). \quad (15)$$

Thus, from (11) and (13), we have

$$g=\frac{A^2\left[1-\exp(-k^2\sigma_0^2/2)\right]^2\sin^2(kx)+\dfrac{I_0+A\sin(kx)}{2\bar{x}}}{I_0+A\sin(kx)}. \quad (16)$$

Or when we consider the mean behavior of $\sigma^2(G\otimes I^*-I^*)$, $\sigma^2(G\otimes\eta)$, and $\sigma^2(\eta)$ over $x\in(-\infty,\infty)$, we have

$$<g>=\frac{A^2}{2I_0}\left[1-\exp(-k^2\sigma_0^2/2)\right]^2+\frac{1}{2\bar{x}}. \quad (17)$$

The optimal σ_0 is obtained when g or <g>is minimal, i.e. $\partial g/\partial\sigma_0=0$ or $\partial<g>/\partial\sigma_0=0$ in (16) or (17).

IV. Results

In this section, we give the comparison of the analytical results with numerical simulations. The Gaussian and Poisson noise series were generated by using Matlab functions random('norm', mean, std) and poissrnd(mean), respectively.

Figure 1 displays σ_r^2 from a Gaussian series with σ =2 and 4 filtered by Gaussian filters with σ_0. Fig. 2 shows σ_r^2 from a Poisson series with noiseless signal $I^*=40$ and 80, and filtered by Gaussian filters. Both figures show that the analytical results (ana2 in the legends) agree with those from numerical simulations. The discrepancy is due to the pixelation of the filter. As σ_0 increases, more pixels are effectively covered within one convolution, resulting in the decrease of the pixilation effect of the filter, and thus the discrepancy decreases. When the value of $2\bar{x}$ is from the pixelated filter, the discrepancy is much smaller (ana1 in the legends). The value of $2\bar{x}$ is from the pixelated filter was calculated as follows.

The pixelated filter

$$f_i=\exp\left[-i^2/(2\sigma_0^2)\right], i=-[5\sigma_0],\ldots,[5\sigma_0]. \quad (18)$$

Then

$$2\bar{x}=\sum_{i=-[5\sigma_0]}^{[5\sigma_0]}(2i+1)f_i\Big/\sum_{i=-[5\sigma_0]}^{[5\sigma_0]}f_i. \quad (19)$$

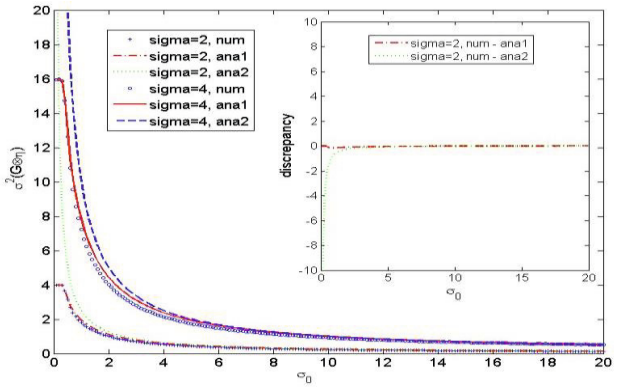

Fig. 1. A comparison of $\sigma^2(G\otimes\eta)$from derived (10) with numerical simulation, where the Gaussian noise has zero mean and standard deviations as indicated in the legend. "num" is for numerical simulation, "ana2" is for analytical result from (11), and "ana1" is for analytical result (10) but $2\bar{x}$ is from (19). The inserted figure displays the difference between the derived and numerical simulation.

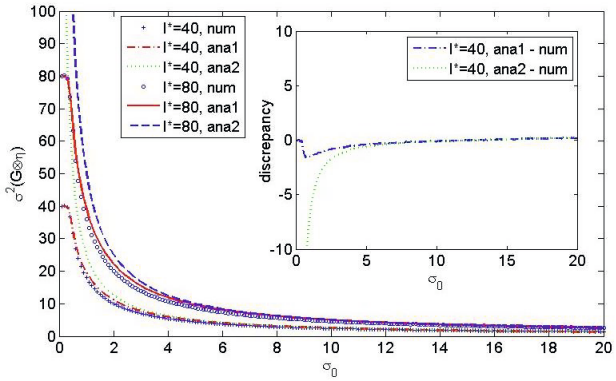

Fig. 2. The same as in Fig. 1 except for Poisson process with the noiseless signal as indicated in the legend.

Figure 3 displays the values of <g>from the analytical result (17) with $2\bar{x}$ calculated from (19), and from the direct simulation on (13), where the Poisson noise was generated with noiseless signal (14). In the numerical simulations, the values of g's over 20 periods of $\sin(kx)$ were averaged. It is seen that the analytical results agree with the numerical simulations, particularly on the optimal σ_0's that correspond to the minimal values of <g>. In addition, the optimal value of σ_0 is more sensitive to k than to A, and so is g. Hence, the multi-scale problem is mainly a multi-resolution issue. Finally, when k is large, <g> is still far away from zero even at optimal σ_0's. This indicates the limitation of multi-scale Gaussian filters.

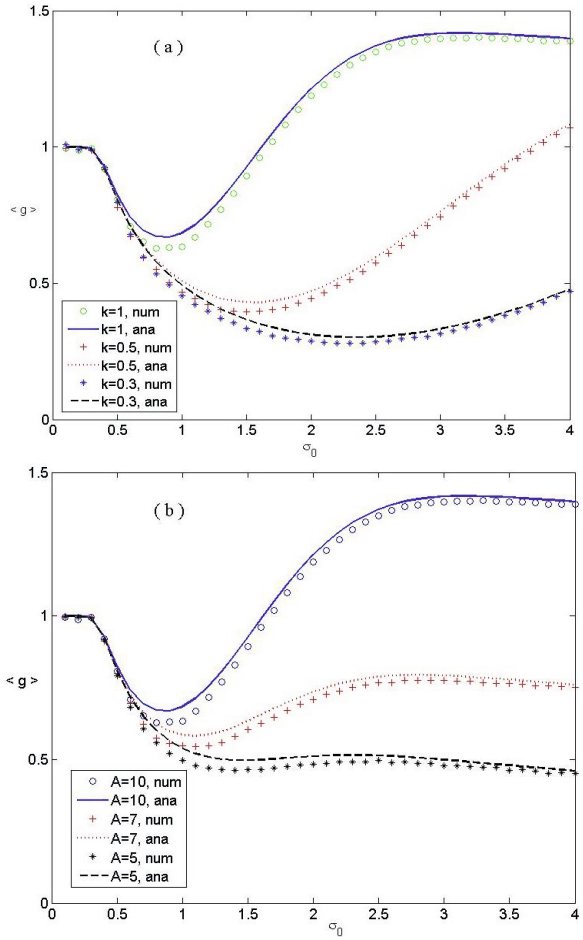

Fig. 3. Comparisons of <*g*>from derivation (17) with numerical simulations of (13) when the noiseless signal is $40 + A\sin(kx), x = 1, 2, 3, \ldots$ (a) A=10 and k=0.3, 0.5 and 1 for simulating different resolutions. (b) k=1 and A=5, 7 and 10 for simulating different contrasts.

V. Conclusions

We have derived analytical forms of the variance of residual noise of Gaussian and Poisson processes after filtered by a Gaussian filter. It is straightforward to extending the derivation to other filters.

We applied the derived forms to determining the optimal variance in the multi-scale Gaussian filters. In real images, such as cone beam CT projections, the value of noiseless signal is not known but may be estimated[3] and then iteratively approached to the expected. Use of analytical form of the variance of residual noise could save the computation and speedup the convergence in the iterative. Furthermore, some optimal noise reduction algorithms such as penalized weighted least-squares method[4,5] often assume some smoothness properties of the noiseless image. These properties could be combined with analytical form of the variance of residual noise to further optimize the parameters in the algorithms.

Conflict of Interest

The authors declare that they have no conflict of interest.

References

1. Tang Z, Hu G. (2010) Development of a Multi-scale Noise Reduction Algorithm for Cone-beam Micro-CT Using Fuzzy Logic-based Anisotropic Filter. J Med Biol Eng 30:283-288
2. Zhu H, Goodyear BG, Lauzon ML et al. (2003) A new local multiscale Fourier analysis for medical imaging. Med Phys 30:1134-1141
3. Starck JL, Murtagh F, and Bijaoui A (1998) Image Processing and Data Analysis: The Multiscale Approach. Cambridge Univ. Press, Cambridge
4. Fessler J (1994) Penalized weighted least-squares image-reconstruction for positron emission tomography. IEEE Trans. Med. Imaging 13:290--300
5. Wang J, Li T, Liang Z and Xing L (2008) Dose reduction for kilovoltage cone-beam computed tomography in radiation therapy. Phys. Med. Biol.53:2897--2909

The address of the corresponding author:

Author: Weiguang Yao
Institute: St. Jude Children's Research Hospital
Street: 262 Danny Thomas Place
City: Memphis
Country: USA
Email: Weiguang.yao@stjude.org